Imaging properties of axicon in a scanning optical system

Rieko Arimoto, Caesar Saloma, Takuo Tanaka, and Satoshi Kawata

The imaging properties of a scanning optical system that incorporates an axicon are presented. Beam-shape characteristics including the axial distribution of the J_0 beam and its control and aberration effects arising from off-axis illumination are experimentally studied. These parameters are relevant when the axicon is used in an imaging system operating in the beam-scanning mode. The J_0 pattern produced by a blazed axicon transmittance grating is also presented.

Key words: Bessel beam, axicon, scanning optics, aberrations, nondiffraction beams.

Introduction

In our last report we proposed the use of an annular pupil in the excitation optics of the laser-scanning fluorescence microscope. A detailed analysis by use of a three-dimensional optical transfer function was carried out.[1,2] The advantage of the use of an annular pupil in the excitation optics is that it provides an extended depth of focus for optical-scanning imaging as well as high lateral resolution, while the annular pupil in the system stops a large amount of the laser beam incident onto the sample, which was an essential disadvantage with this idea. In this paper we describe the introduction of an axicon (conical prism) into the optical system instead of an annular pupil. The axicon with the Fourier transform lens forms an annular pattern without energy loss of light by a beam stop.

The imaging properties with the axicon were investigated originally by McLeod in 1954 before the laser was developed. (The name axicon also originated with him.[3]) The axicon was used as an optical element producing a circle with a Fourier transform lens in laser machining as early as 15 years ago[4,5] because of its ability to deliver a large amount of confined energy inside a ring pattern. Just recently this advantage has been employed in corneal surgery.[6] Another application of the axicon was found recently in the laser beam collimator of Čerenkov radiation from the second-harmonic generator of a laser diode.[7] The narrower central spot that is available over long axial distances was used in aligning and trapping atoms along the axis with the use of laser-trapping technology.[8]

In the mean time Durnin et al.[9,10] reported the nondiffractive propagation nature of the laser beam, which is given by Bessel functions, particularly the J_0 (zero-order Bessel) beam as the simplest form. Since the J_0 beam is the Fourier transform of a ring with an infinitively thin width, it can be realized at the back focal plane of a lens with a thin annular pupil at the front focal plane.

The conical surface of an axicon generates the J_0 beam with on-axis illumination, as was first shown by Fujiwara.[11] The axicon provides the most efficient (throughput-advantageous) method of realizing generally diffractionless beams. For a given aperture the diameter of the central spot of the $|J_0|^2$ beam is narrower than the first dark ring of the Airy disk pattern by $\sim 38\%$ for an infinitely small annular width.[12] This promises superresolution in imaging. In this paper we investigate the imaging properties of the axicon that is crucial in applications to scanning optical systems. We found that an axicon easily succumbs to aberration in the case of oblique illumination. Knowledge of the aberration and its correction is essential in designing a scanning imaging system. A measurement of the axial intensity distribution of the J_0 beam is also presented.

Optics and Aberration

In Fig. 1 the intensity distribution at point P(x, y, z) owing to an axicon of radius R_0 that is illuminated by a plane wave incident upon its facet (stationary phase
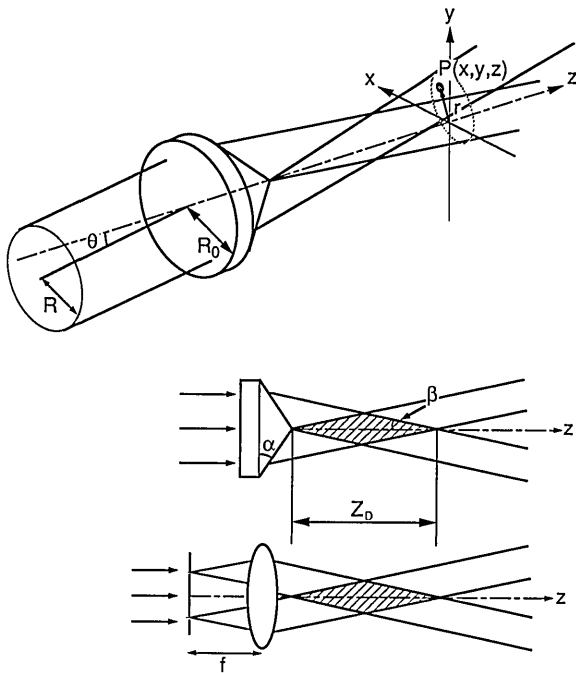
Fig. 1. Geometry of an axicon during the J_0 beam production and the equivalent optics of an annular pupil with a lens to the axicon.

approximation) is[13]

$$I(r, z) = \frac{4\pi^2 E^2(R)}{\lambda} \frac{R \sin \beta}{\cos^2 \beta} J_0^2 \left(\frac{2\pi r \sin \beta}{\lambda} \right),$$

$$z \le z_D \text{ and } R \le R_0, \qquad (1)$$

where $E^2(R)$ is the incident energy of the incident beam of radius R, i.e., $[E_{max} = E(R_0)]$, $r^2 = x^2 + y^2$ is evaluated on the observation plane z, and λ is the wavelength of the illumination. The angles α and β and the depth of focus of the axicon z_D are subject to the following constraints:

$$n \sin \alpha = \sin(\alpha + \beta), \qquad (2a)$$

$$z_D = R(\cot \beta - \tan \alpha), \qquad (2b)$$

where n is the refractive index of the axicon and β corresponds to the numerical aperture of the axicon. The central spot has a radius of $0.383\lambda/\beta$. Equation (1) is applicable only to the normal incidence, i.e., when the infinitely distant-point light source is located on the z axis ($\theta = 0$ in Fig. 1). Oblique illumination results in an aberrated image of the point source with the central spot and the inner sidelobes of the J_0 beam most easily affected. The equivalent optics of an annular pupil with a lens to the axicon is shown at the bottom of Fig. 1.

Figure 2 shows a series of images caused by the oblique plane-wave illumination ($\lambda = 488$ nm, argon-ion laser) at various angles θ (degrees) of incidence: $\theta = 0$, $\theta = 1$, $\theta = 1.5$, and $\theta = 2$. We viewed the images using a microscope (400× magnification) and a CCD camera (Sony XC-77, 768 × 493 pixels; pixel dimensions, 11 × 13 μm) with the observation plane
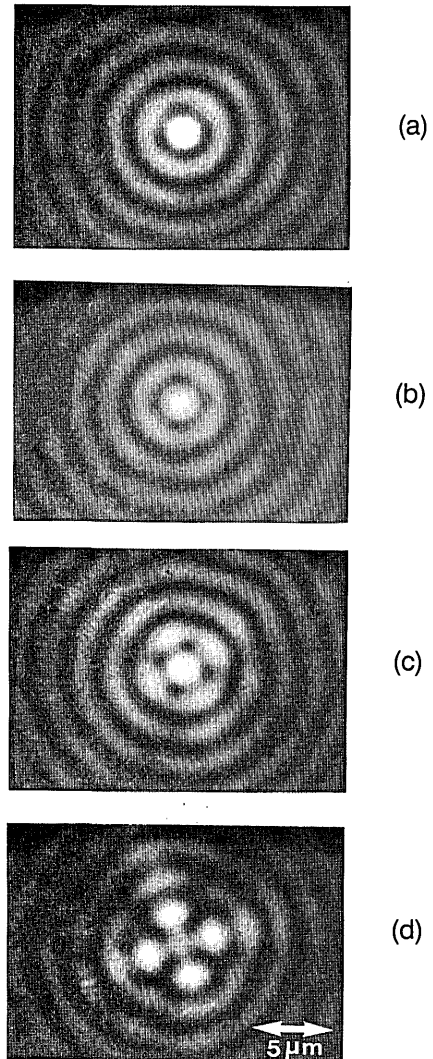

Fig. 2. Far-field pattern produced by an axicon at $z = 32.1$ mm: (a) $\theta = 0$ deg, (b) $\theta = 1$ deg, (c) $\theta = 1.5$ deg, and (d) $\theta = 2.0$ deg. (The peak of the spot on the photograph is saturated to make the first ring appear.)

at $z = 32.1$ mm. The axicon parameters were: $n = 1.522$ (BK7), $\alpha = 10$ deg, and $R_0 = 5$ mm. An 8-bit frame grabber (Shibasoku) was used to transport the image into a microcomputer. The peak of the spot on the photograph is saturated to make an appearance on the first ring. The intensity of the first ring is one sixth of the peak.

The deviations in the patterns exhibit symmetry and are, therefore, characterized by an even-ordered aberration, primarily astigmatism, but not coma. The reason the system using an annular pupil is insensitive to coma can be explained as follows. Coma is a wave-front aberration of the form $r^3 \cos \theta$, where r is the pupil radius and θ is the polar angle. If r is held constant, as is the case for the annular aperture, the effect of coma is simply to add a tilt term to the wave front, which has no effect on the shape of the spot.

While a rigorous analytical solution to the image amplitude distribution for oblique illumination is

forbidding, insight into the particular nature of the aberration can be gained by noting that the result produced by the method of stationary phase (first order) is identical with that by the method of the Fresnel zone.[14] Thus the result given by Eq. (1) may be obtained also by solving the Kirchhoff integral for the image amplitude with the area of integration restricted to lie within an annulus of width $\sqrt{\lambda z}$ and a center-line radius equal to $\alpha(n-1)z$.

When the illumination is off axis, the annular Fresnel zone loses width uniformity and eventually deteriorates into two separated crescent-shaped zones. As a result the amplitude contributions from various regions in the zone into the observation point $P(x, y, z)$ are no longer uniform. The far-field distribution at the observation plane located at z, which can be calculated as the Fourier transform of the first Fresnel zone, is no longer amply described by a zero-order Bessel function but rather by the linear superposition of weighted higher-order Bessel functions. Its corresponding pattern is not circularly symmetric in the x-y plane and does not reveal a circular central spot. However, the propagation distances of these patterns are extremely long with the weakly aberrated ones having a depth of focus that is approximately equal to that of the J_0 beam.

Even with on-axis plane-wave illumination an axicon with an imperfect conical surface, e.g., one with its surface warped about the optical axis, also exhibits the same type of aberration since the shape of its first Fresnel zone no longer typifies a perfect annulus.[15]

Depth of Focus

The depth of focus z_D defined as the distance from the axicon apex to the edge of the geometrical shadow for full-facet illumination is given by Eq. (2b) for $R = R_0$. For small $\alpha[\alpha = 0.17$ rad ($=10$ deg) is considered small] the depth simplifies to

$$z_D = \frac{R_0}{(n-1)\alpha}. \tag{3}$$

Thus we can regulate the depth of focus by placing a variable aperture in front of the axicon facet. The depth changes linearly with the aperture radius. Within the depth of focus the peak intensity of the central spot oscillates and rapidly decays at the end of the depth of focus. Figure 3 shows the axial intensity distribution of the peak of the central spot of the J_0 beam. (The theoretical depth of focus is 54.89 mm.) Consistent with the theoretical prediction,[9] the intensity oscillated increasingly along the z axis attaining a maximum value about a value equal to $4\lambda^{-1}\pi^2(n-1)\alpha^2 z^2$ before rapidly decaying after the geometrical shadow.[16] This variation in the axial intensity may be utilized to select a particular strength for the central spot. The amplitude of the axial oscillation decreases for axicons with larger facet radii.

Beam Scanning and Aberration

Figure 4 displays our setup of the beam-scanning imaging system with an axicon. The same axicon
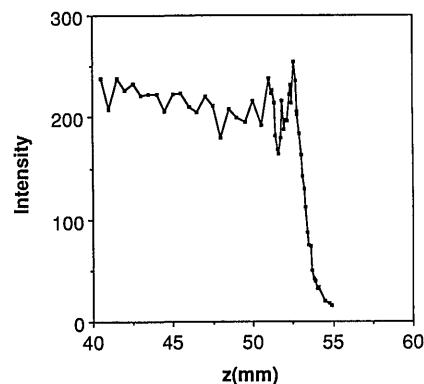

Fig. 3. Peak intensity distribution of the J_0 beam central spot inside the depth of focus.

that we used to obtain Figs. 2 and 3 was used to form a J_0 function source pattern in the primary source plane; the lens L1 (focal length $f_1 = 80$ mm; diameter, 30 mm) takes the Fourier transform of the J_0 to provide an annulus on the mirror M. The radius of the annulus on the mirror M is given by $(n-1)\alpha f_1$. Beam scanning at the sample plane was accomplished by rotating mirror M. Lens L2 (a biconvex singlet) images the J_0 Bessel beam at its focal place (the secondary source plane) and the ring at the pupil plane (the conjugate plane of the mirror M). Finally the objective lens reconstructs the moving J_0 beam in the sample plane according to the mirror rotation.

Figure 5 illustrates the evolution of the J_0 beam in the secondary source plane with mirror rotation. The central spot in pattern A located on the optical axis of L2 corresponds to the null angular displacement of the mirror, $\theta = 0$. Patterns B–D resulted
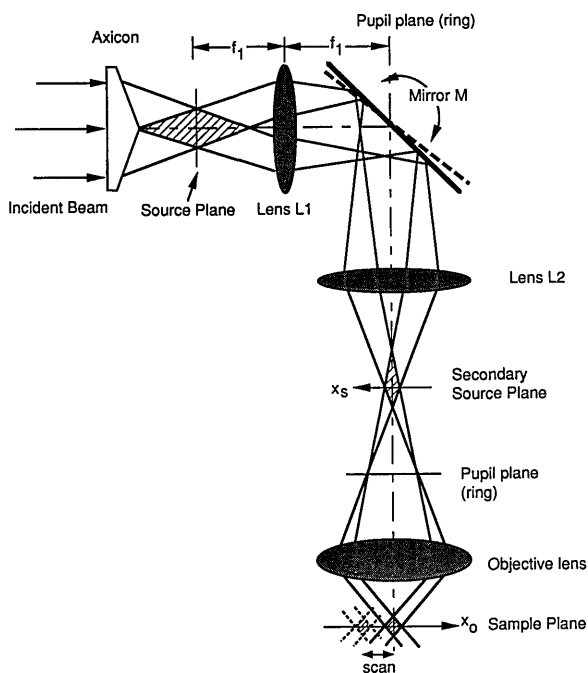

Fig. 4. Beam-scanning imaging using an axicon as a generator of the primary light source.
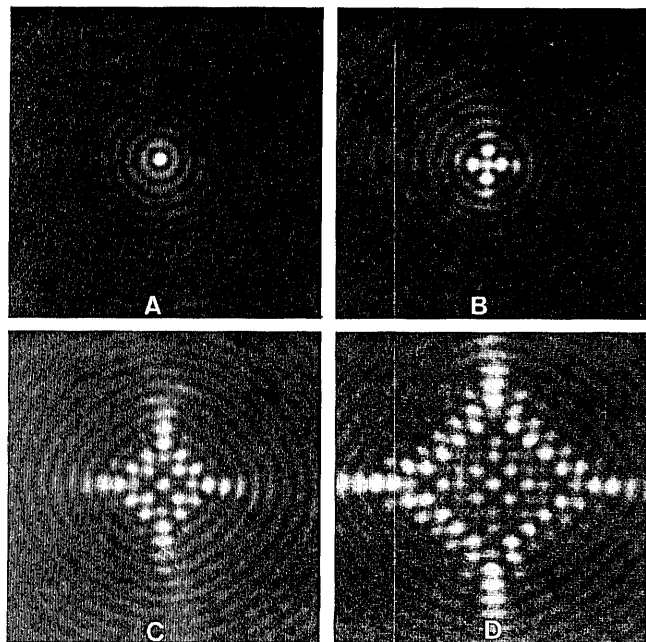
Fig. 5. Evolution of the J_0 beam in the secondary source plane resulting from the mirror scan: θ = 0; B, θ = 1.0 deg; C, θ = 2.0 deg; D, θ = 3.0 deg. The intensity of each pattern is normalized by its maximum intensity.

Fig. 6. Same result as shown in Fig. 6 but with an aberration-corrected lens for L2.

from displacements from the optical axis as a result of the mirror rotation equal to θ = 1.0, θ = 2.0, and θ = 3.0 deg, respectively. The intensity of each pattern is normalized by its maximum intensity. The image patterns increasingly display astigmatism and degradation of the circular central spot with increasing rotation of the mirror. The degradation of the circular central spot with mirror rotation arose from the apparent deterioration (from the point of view of L2) of the annular ring into one with an elliptical perimeter and nonuniform width.

The maximum scanning range (field of view) x_s was limited by the lens aberration of L2 because of the off-axis imaging of the ring about the optical axis resulting from the tilting of the mirror. Images uncorrupted by aberrations may be obtained by employing sample scanning instead of beam scanning but at a reduced sampling rate.

Figure 6 shows the same result as Fig. 5 but with an aberration-corrected lens (camera lens with f = 1.4) for L2. The spot distortion was well corrected in Fig. 6 for the tilting mirror arrangement compared with the results in Fig. 5. This means that the heavy spot distortion in Fig. 5 was due to the lens aberration of L2. For laser-scanning microscopy we have to choose carefully or redesign a lens to cover a wide scanning field of view.

Axicon Grating

The axicon belongs to a family of conical surfaces that are capable of producing a J_0 beam. An axicon (circular) phase grating that is blazed to attain better coupling efficiency also generates a J_0 beam (see Fig. 7). In Figs. 8(a) and 8(b) are patterns produced by
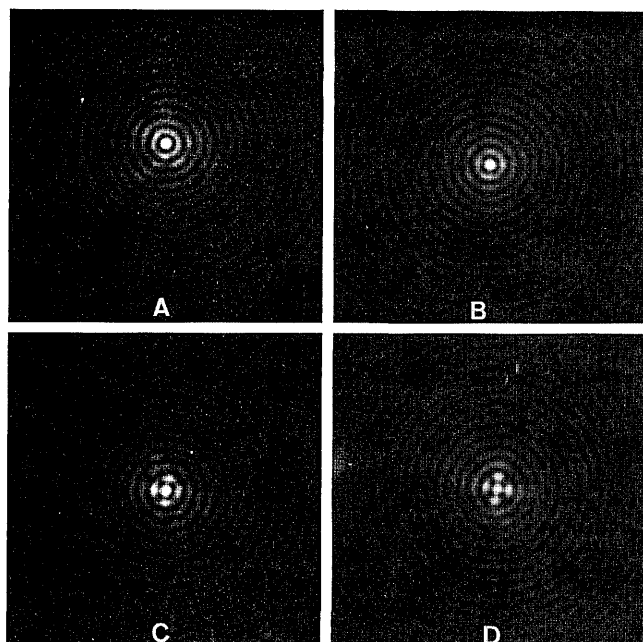
such a transmittance-type grating (the substrate is SiO_2) with the following dimensions: groove period, 4.79 μm; diameter, 4 mm; blazed angle, 7.30 deg. Figure 8(a) corresponds to a normal plane-wave illumination, while Fig. 8(b) is an aberrated pattern resulting from a slight off-axis illumination. The functional forms of both patterns are the same as those that are produced when the axicon is used.

Discussion

The imaging properties of the axicon in a beam-scanning imaging system were discussed with experi-
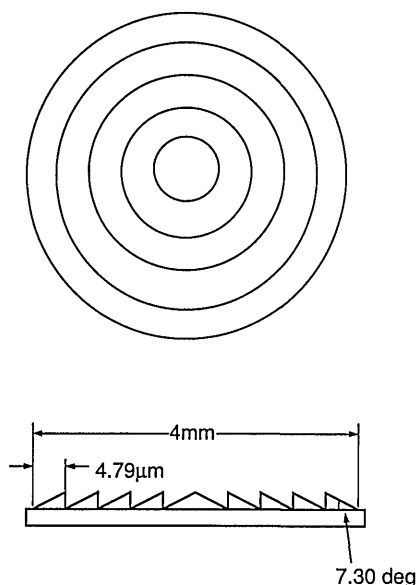

Fig. 7. Geometry of a blazed axicon grating (transmittance type: line spacing, 4.79 μm; diameter, 4 mm; blazed angle, 7.30 angle).
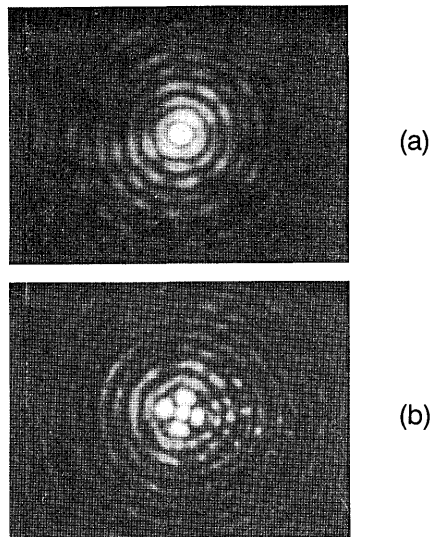
Fig. 8. Intensity distribution of a J_0 beam produced by a blazed axicon grating: (a) normal incidence; (b) off-axis illumination.

mental results. The advantages of a narrower central spot and long depth of focus with axicon imaging could be utilized in the configuration of a scanning imaging system where the image is realized point by point.

The advantage of a narrower central spot may be compromised by the high strengths of the accompanying sidelobes of the J_0 beam, which results in low-contrast images. However, this can be rendered ineffectual during applications in laser-scanning imaging, optical memory, laser-beam trapping, or photolithography by applying to photoresists or fluorescent samples or other materials with nonlinear responses or the threshold responses that are higher than the peak strengths of the sidelobes.

We are now constructing a video rate laser-scan microscope equipped with an axicon, where a rapidly rotating multifaceted polygon mirror with a 15-kHz horizontal scan and a galvanomirror with a 60-Hz vertical scan are used. Since the axis of rotation of the polygon is not in the plane of the facets it would seem that the pupil will move side to side as the polygon rotates. This would be another problem that we have to solve in the future.

References

1. R. Arimoto and S. Kawata, "Laser-scan fluorescence microscope with annular excitation," Optik (Stuttgart) 86, 651–654 (1990).
2. S. Kawata, R. Arimoto, and O. Nakamura, "Three-dimensional optical-transfer-function analysis for a laser-scan fluorescence microscopy," J. Opt. Soc. Am. A 8, 171–175 (1991).
3. J. H. McLeod, "The axicon: a new type of optical element," J. Opt. Soc. Am. 44, 592–597 (1954).
4. P. A. Belanguer and M. Rioux, "Ring pattern of lens–axicon doublet illuminated by a Gaussian beam," Appl. Opt. 17, 1080–1086 (1978).
5. M. Rioux, R. Tremblay, and P. A. Belanguer, "Linear, annular, and radial focusing with axicons and applications to laser machining," Appl. Opt. 17, 1532–1536 (1978).
6. Q. Ren and R. Birngruber, "Axicon: a new laser beam delivery system for corneal surgery," IEEE J. Quantum Electron. 26, 2305–2308 (1990).
7. S. Okamoto, K. Chikuma, T. Tohma, and S. Umegaki, "Focussing system of optical second harmonic wave from crystal cored fiber," in Proceedings of the Semiannual Meeting of the Japanese Society of Applied Physics (Fukuoka, Japan, 1989), p. 923.
8. V. I. Balykin, V. S. Letokhov, V. G. Minogin, Yu. V. Rozbdestvenskyt, and A. L. Sidorov, "Radiative collimation of atomic beams through two-dimensional cooling of atoms by laser-radiation pressure," J. Opt. Soc. Am. B 2, 1776–1783 (1985).
9. J. Durnin, "Exact solutions for non-diffracting beams. I. The scalar theory," J. Opt. Soc. Am. A 4, 651–654 (1987).
10. J. Durnin, J. Miceli, Jr., and J. Eberly, "Diffraction-free beams," Phys. Rev. Lett. 58, 1499–1501 (1987).
11. S. Fujiwara, "Optical properties of conic surfaces: I. reflecting cone," J. Opt. Soc. Am. 52, 287–292 (1962).
12. M. Born and E. Wolf, Principles of Optics (Pergamon, New York, 1989), pp. 416–417.
13. R. Herman and T. Wiggins, "Production and uses of diffractionless beams," J. Opt. Soc. Am. A 8, 932–942 (1991).
14. N. G. Van Kampen, "The method of stationary phase and the method of Fresnel zones," Physica 24, 437–444 (1958).
15. J. H. MacLeod, "Axicon and their uses," J. Opt. Soc. Am. 50, 166–169 (1960).
16. M. V. Perez, C. Gomez-Reino, and J. Cuadrado, "Diffraction patterns and zone plates produced by linear thin axicons," Opt. Acta 33, 1161–1176 (1986).